Design of Single Angles Bent About the Major Principal Axis

CHRISTOPHER J. EARLS

Hot rolled steel angles are frequently used in applications wherein their flexural strength must be quantified. While flexural applications of angle members frequently involves bending within the plane of one of the angle legs, other bending scenarios can arise. One other similar scenario involves bending a single angle member about its major principal centroidal axis as shown in Figure 1. A practical example of when this type of bending may occur involves the case of sign and billboard structures in which an equal leg single angle member may be specified for the girts that support the face of the sign. The effects of gravity loading from the face of the sign result in major axis bending of the girts. In such instances it is obviously important to understand the major axis strength characteristics of the single angle members.

Other instances of single angle bending, wherein flexure occurs about the major principal axis, can be found in the supporting structure of duct work and machinery, in the design of stairs, and in the proportioning of elements in hoppers and industrial rack systems. Furthermore, the major principal axis flexural capacity must also be known for applications involving single angles whose design is governed by the bi-axial interaction expressions frequently used in governing design specifications.

While design specifications providing guidance for the proportioning of equal leg single angle components bent about the major principal axis exist, they are frequently cumbersome to apply and, as in the case of the American, Australian, and British specifications (AISC, 2000; SA, 1998; BSI, 2000), are overly conservative (as pointed out in recent research (Earls, 1999a; Trahair, 2002)). More easily applied design recommendations, that result in designs with less conservatism than is presently the case, would be an improvement in the situation that many designers currently face when proportioning single beams bent in the fashion under discussion.

Christopher J. Earls is associate professor and William Kepler Whiteford Faculty Fellow, department of civil and environmental engineering, University of Pittsburgh, Pittsburgh, PA.

Earlier research related to the current topic is contained in the report by Trahair (2002). Trahair investigated the elastic response (considering both small and large cross-sectional rotations) of unequal leg, unbraced single angle beams bent about the major principal axis of the cross-section. Despite a strictly elastic analytical approach, Trahair was able to formulate a design methodology that he lays out in Section 3 of the referenced report. The present research takes a different analytical approach from that of Trahair in that the current results are obtained using a nonlinear finite element approach that overtly considers both geometric and material nonlinearities.

Scope

The current research focuses on equal leg single angles bent about the major principal centroidal axis (see Figure 1). The applied moment is constant along a test section that is part of a three segment simply-supported flexural configuration in which the properties of the two end segments, adjoining the central test region, are essentially rigid. A schematic representation of the problem geometry is presented in Figure 2.

All angles considered as part of the present research are made from hot-rolled steel. Despite the sometimes very high yield strengths considered in this work, mild carbon steel best describes the type of steel considered; based on

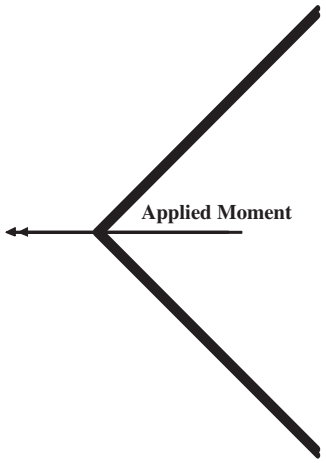

Fig. 1. Flexure about the major principal centroidal axis.

the yield plateau length and strain-hardening slope. Four distinct yield stresses of this steel type are studied herein: 276 MPa, 345 MPa, 414 MPa, and 483 MPa. The inelastic portion of the constitutive response is held constant over variations in yield stress. Thus, as a change in yield stress occurs, the plastic plateau and strain hardening region simply slide up or down along a line whose slope is the initial material stiffness as shown in Figure 3.

FINITE ELEMENT MODELING TECHNIQUES

The commercial multipurpose finite element software package ABAQUS (1999) is employed in this research. All modeling reported herein considers both nonlinear geometric and material influences. The incremental solution strategy chosen for this work is the modified Riks-Wempner method (ABAQUS, 1999).

Modeling Overview

The models of the single angle beams considered herein are constructed from a dense mesh of nine node shell finite elements. The planes of the mesh surfaces correspond with the middle surfaces of the constituent single angle cross-sectional plate components (see Figure 4). A constant moment loading is used in this study since it represents the most severe flexural condition for single angle beams and as such represents the loading case that is explicitly treated in the development of design specification equations for nominal moment capacity. This constant moment loading is achieved by applying concentrated forces perpendicular to the beam longitudinal axis at two points on a simply-supported span as depicted in Figure 2. The concentrated forces are applied to the single angle shear center so as not to induce a primary torsional loading of the beams. Both end segments of the model experience a less critical moment gradient loading and hence the precise response in these end segments is not at issue, thus they are modeled with a coarser mesh than that of the central segment of the beam. In the central region of the beam, high mesh densities are used in order that phenomena such as localized buckling may be allowed to develop in the model. Inter-element compatibility within the graded mesh is ensured at the mesh transition interfaces through the use of the ABAQUS Multi-Point Constraint feature (ABAQUS, 1999). Restraint against out-of-plane translation is enforced at all nodes along the interfaces between the rigid and flexible segments. As a result of this out-of-plane restraint, torsional restraint is also provided at the bracing location. Furthermore, as a result of the rigid end sections, these same locations also experience a restraint of warping deformations.

The ABAQUS S9R5 nonlinear shell finite element is used for all modeling reported here. The S9R5 shell element is shear deformable and subsequently both reduced integration and discrete Kirchhoff theory are employed to improve the overall thin-shell behavior of the element. A 2x2 Gauss quadrature is used in-plane and the discrete Kirchhoff condition is imposed at a finite number of points on the shell reference surface by way of a penalty function (ABAQUS, 1999). In general, the S9R5 formulation is considered to be a large displacement, small strain type formulation. Despite the fact that this element is formulated for small strain applications, it nonetheless performs quite well in applications requiring the correct modeling of moderate to large strain behavior as evidenced by experimental verification associated with similar problems to those treated herein (Earls, 2001a; Earls, 2001b; Earls, 2001c; Earls, 2001d).

A uniaxial representation of the constitutive law employed in this study appears in Figure 5 as a plot of true

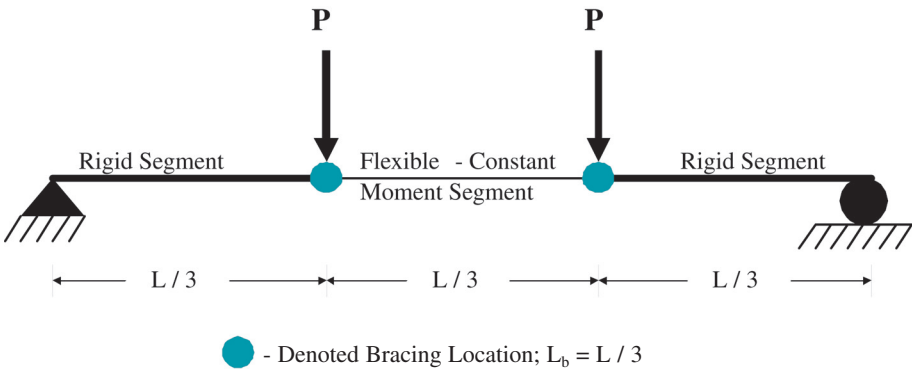

Fig. 2. Schematic of global specimen geometry.

stress versus logarithmic strain. This piece-wise linear model has a yield stress that varies as a parameter of the study. The ratio F_u / F_y also varies within the study, but in all cases $\varepsilon_u / \varepsilon_y = 45$ and $\varepsilon_{st} / \varepsilon_y = 5.5$. ABAQUS uses the von Mises yield criterion to extrapolate a yield surface in three-dimensional principal stress space from the uniaxial material response given above. The corresponding ABAQUS metal plasticity model is characterized as an associated flow plasticity model incorporating isotropic hardening. It is noted that residual stresses are not considered in the present study since their influence on the structural response, at ultimate load, of hot-rolled angle beams tends to be insignificant (Earls, 1999b).

Geometric Imperfections

In modeling studies where inelastic buckling is considered, it is important that the evolution of the analytical solution be carefully monitored so that any indication of bifurcation in the equilibrium path is carefully assessed so as to guarantee that the equilibrium branch being followed corresponds to the lowest energy state of the system. The strategy of seeding the finite element mesh with an initial displacement field is employed in this study (ABAQUS, 1999) as means of helping to ensure that the practically meaningful equilibrium branch is followed. In such a technique, the finite element mesh is subjected to a linearized-eigenvalue buckling analysis from which an approximation to the first buckling mode of the angle beam is obtained. The displacement field associated with this lowest mode is then superimposed on the finite element model as a seed imperfection in the fully nonlinear analysis. This seed imperfection field is scaled so that the maximum initial displacement anywhere in the mesh is equal to one-one-thousandth of the maximum unbraced length of the angle (L_b / 1000), a value consistent with the AISC Code of Standard Practice (AISC, 2000). While it is recognized that the technique of seeding a finite element mesh with an initial imperfection has shortcomings, this technique is nonetheless employed in the current study due to the fact that results obtained from this method have agreed quite well with experimental tests obtained from the single angle literature (Earls, 2001a; Earls, 2001b; Earls, 2001c; Earls, 2001d).

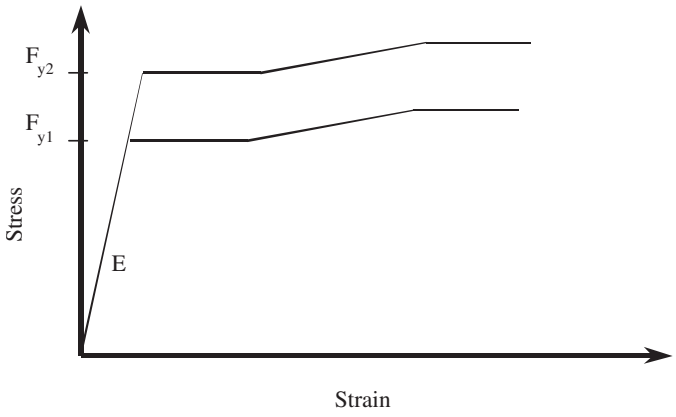

Fig. 3. Assumed inelastic behavior as yield stress varies.

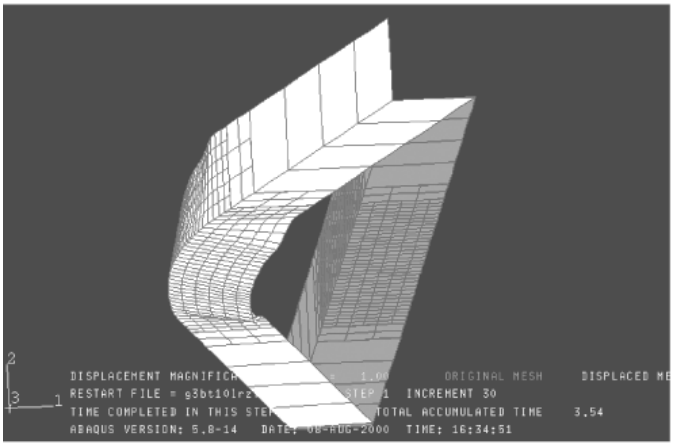

Fig. 4. Representative finite element mesh.

RESULTS

Finite element studies of 128 different major axis single angle flexural cases are considered herein. This test population spans four different steel grades (276 MPa, 345 MPa, 414 MPa, and 483 MPa), eight different plate slenderness values of the angle legs (b/t = 6, 8, 10, 12, 14, 16, 18, and 20), and four different beam slenderness values (L_b / r_z = 50, 100, 150, and 200). The results from the analyses of these

Uniaxial Material Response

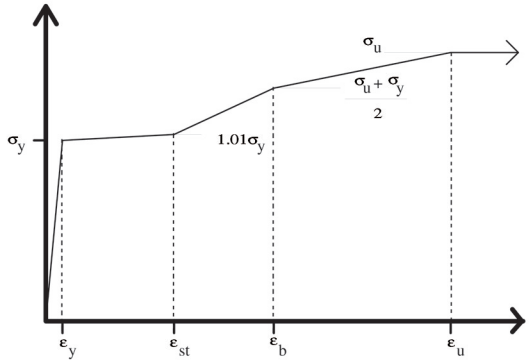

Material	σ_y	σ_u / σ_y	$\varepsilon_{st} / \varepsilon_y$	$\varepsilon_b / \varepsilon_y$	$\varepsilon_u / \varepsilon_y$
Medium Carbon Steel	F_y	*Varies with* F_y	*5.5*	*28*	*45*

Fig. 5. Uniaxial representation of constitutive model.

128 cases are summarized in Table 1 and in Figures 6 through 12.

It is noted that in Table 1 and Figures 6 through 12, an angle flexural strength in excess of the ideal plastic capacity is not reported. While a large number of the single angles in the present test population were able to exceed this theoretical capacity, (as a result of material strain hardening) it was felt that a practical limit on the cross-sectional capacity corresponding to a shape factor of 1.5 was best adopted so as to allay concerns surrounding the possibility of excessive cross-sectional distortion occurring at the large rotations needed to attain ultimate moments in excess of the theoretical.

Discussion of Results

While Table 1 shows that at $b/t = 6$, all steel grades considered herein yield a capacity that at least achieves the ideal theoretical plastic capacity for all four of the beam slendernesses considered, the same is not true for the remaining 112 cases. In these other cases, the nominal angle moment capacity tended to be attenuated by increasing steel strength, increasing plate slenderness of the legs, and increases in beam slenderness. While the exact relationship governing the simultaneous influences of all three of these parameters on the observed nominal moment capacity is difficult to precisely quantify, an approximate approach is adopted in the present work for the purposes of identifying a reasonably simple and accurate design methodology. In this approach, the data population is considered on a case-by-case basis, as delineated by plate slenderness value (b/t) of the angle leg. At a given plate slenderness value, the data are examined so as to identify two lower-bound ordered pairs, of steel grade and beam slenderness, that span the

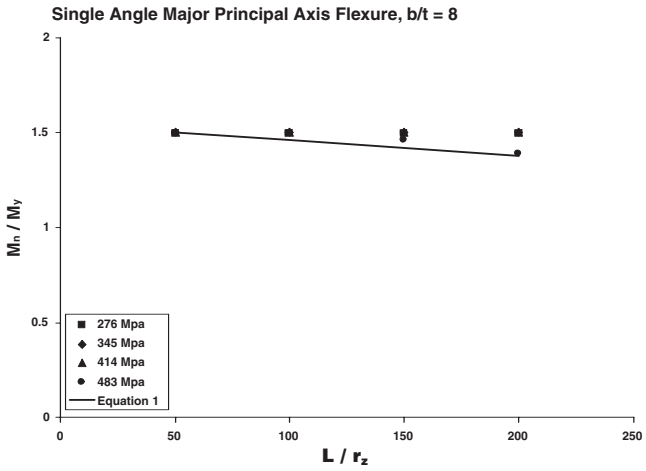

Fig. 6. Finite element results plotted with proposed predictive equation.

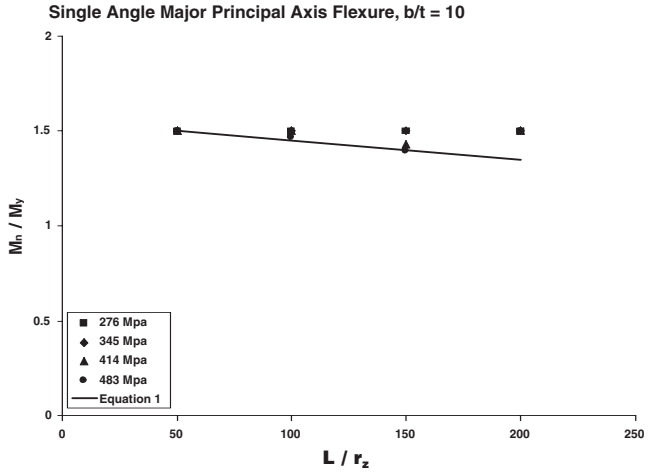

Fig. 7. Finite element results plotted with proposed predictive equation.

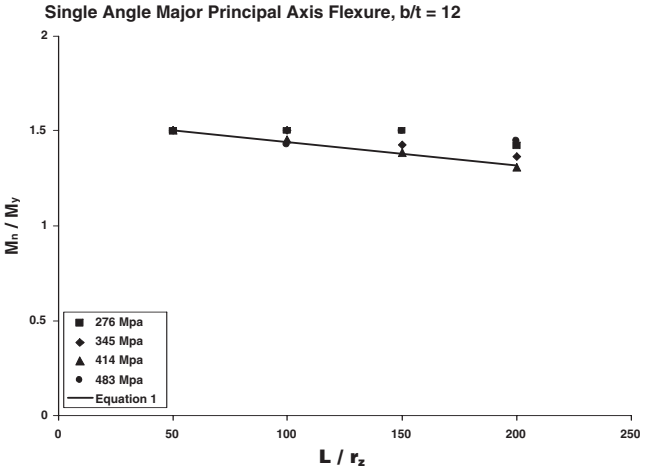

Fig. 8. Finite element results plotted with proposed predictive equation.

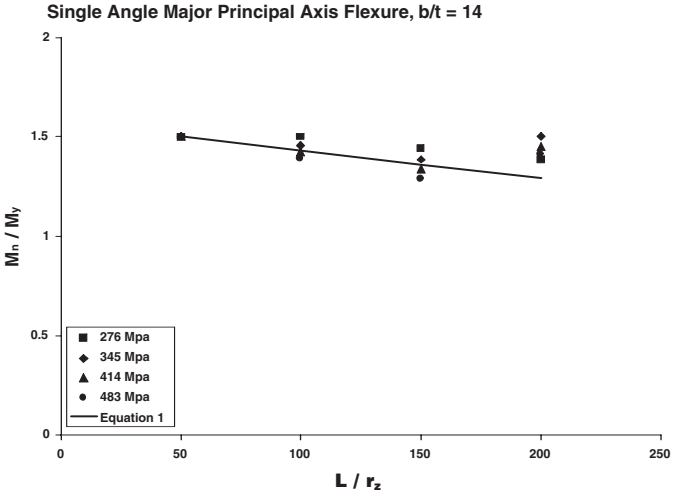

Fig. 9. Finite element results plotted with proposed predictive equation.

Table 1. Analysis Results

M_n / M_y				
$b / t = 6$	$L_b / r_z = 50$	$L_b / r_z = 100$	$L_b / r_z = 150$	$L_b / r_z = 200$
$F_y = 276$ MPa	1.5	1.5	1.5	1.5
$F_y = 345$ MPa	1.5	1.5	1.5	1.5
$F_y = 414$ MPa	1.5	1.5	1.5	1.5
$F_y = 483$ MPa	1.5	1.5	1.5	1.5

M_n / M_y				
$b / t = 8$	$L_b / r_z = 50$	$L_b / r_z = 100$	$L_b / r_z = 150$	$L_b / r_z = 200$
$F_y = 276$ MPa	1.5	1.5	1.5	1.5
$F_y = 345$ MPa	1.5	1.5	1.5	1.5
$F_y = 414$ MPa	1.5	1.5	1.5	1.5
$F_y = 483$ MPa	1.5	1.5	1.459	1.389

M_n / M_y				
$b / t = 10$	$L_b / r_z = 50$	$L_b / r_z = 100$	$L_b / r_z = 150$	$L_b / r_z = 200$
$F_y = 276$ MPa	1.5	1.5	1.5	1.5
$F_y = 345$ MPa	1.5	1.5	1.5	1.5
$F_y = 414$ MPa	1.5	1.5	1.432	1.5
$F_y = 483$ MPa	1.5	1.466	1.395	1.5

M_n / M_y				
$b / t = 12$	$L_b / r_z = 50$	$L_b / r_z = 100$	$L_b / r_z = 150$	$L_b / r_z = 200$
$F_y = 276$ MPa	1.5	1.5	1.5	1.420
$F_y = 345$ MPa	1.5	1.5	1.424	1.365
$F_y = 414$ MPa	1.5	1.454	1.383	1.308
$F_y = 483$ MPa	1.5	1.427	1.5	1.448

Table continued on next page.

Table 1. Analysis Results (continued)

	M_n / M_y			
b / t = 14	$L_b / r_z = 50$	$L_b / r_z = 100$	$L_b / r_z = 150$	$L_b / r_z = 200$
F_y = 276 MPa	1.5	1.5	1.439	1.383
F_y = 345 MPa	1.5	1.458	1.387	1.5
F_y = 414 MPa	1.5	1.423	1.338	1.449
F_y = 483 MPa	1.5	1.389	1.286	1.411

	M_n / M_y			
b / t = 16	$L_b / r_z = 50$	$L_b / r_z = 100$	$L_b / r_z = 150$	$L_b / r_z = 200$
F_y = 276 MPa	1.5	1.463	1.403	1.5
F_y = 345 MPa	1.5	1.430	1.346	1.260
F_y = 414 MPa	1.453	1.387	1.286	1.407
F_y = 483 MPa	1.388	1.347	1.408	1.112

	M_n / M_y			
b / t = 18	$L_b / r_z = 50$	$L_b / r_z = 100$	$L_b / r_z = 150$	$L_b / r_z = 200$
F_y = 276 MPa	1.5	1.446	1.5	1.465
F_y = 345 MPa	1.449	1.397	1.305	1.417
F_y = 414 MPa	1.343	1.343	1.237	1.122
F_y = 483 MPa	1.267	1.260	1.174	1.259

	M_n / M_y			
b / t = 20	$L_b / r_z = 50$	$L_b / r_z = 100$	$L_b / r_z = 150$	$L_b / r_z = 200$
F_y = 276 MPa	1.454	1.420	1.338	1.254
F_y = 345 MPa	1.340	1.343	1.264	1.163
F_y = 414 MPa	1.273	1.220	1.190	1.069
F_y = 483 MPa	1.127	N.A.	1.112	N.A.

design space under investigation. A linear variation in nominal moment capacity as a function of beam slenderness is then assumed in the formulation of the proposed equations for the prediction of nominal moment. The linearity of this relationship is hinted at in the form of the plotted data obtained from the finite element modeling. Two different design equations are being proposed herein as a result of the fashion in which the data present themselves in Table 1. While both of the proposed predictive equations are linear, the second equation has a larger negative slope than the first.

Proposed Nominal Moment Predictive Equations

Based on the observed trends in the data corresponding to each angle leg plate slenderness value, linear expressions relating nominal moment capacity and beam slenderness are arrived at using the data points related to a lower bound of the test population (irrespective of steel grade). The results of this exercise are presented below in the form of Equations 1 and 2. The conservatism of these equations can be observed in the plots presented in Figures 6 through 12.

For $8 \le b/t \le 14$,

$$\frac{M_n}{M_y} = -\frac{b/t}{10,000}\left(\frac{L_b}{r_z} - 50\right) + 1.5 \qquad (1)$$

and for $b/t > 14$,

$$\frac{M_n}{M_y} = -0.00184\left(\frac{L_b}{r_z} - 50\right)\left(\frac{16}{b/t}\right)^7 + \left(\frac{22.4}{b/t}\right) \qquad (2)$$

It is pointed out that in the above equations a unit effective length factor is implied for the unbraced length, L_b. While in a purely elastic analysis, one might apply an effective length factor of ½ to the unbraced lengths considered (due to the degree of fixity against cross-sectional twist and out-of-plane bending) (Galambos, 1968; Vlasov, 1959; Trahair, 1993), the same is not true for inelastic flexural buckling in angles as recently pointed out (Earls, 2002). Due to the nature of single angle inelastic buckling phenomena, a stocky angle beam displays a significantly different buckling mode than that of a more slender angle beam having the exact same boundary conditions; vis-à-vis the location of the points of inflection in the observed buckling mode. It is then recognized that since there is no universality in the location of the points of inflection in the mode shapes of single angle beams with identical boundary conditions,

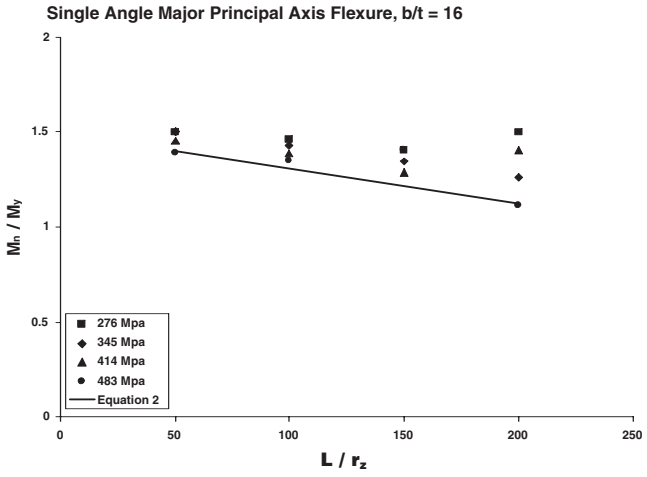

Fig. 10. Finite element results plotted with proposed predictive equation.

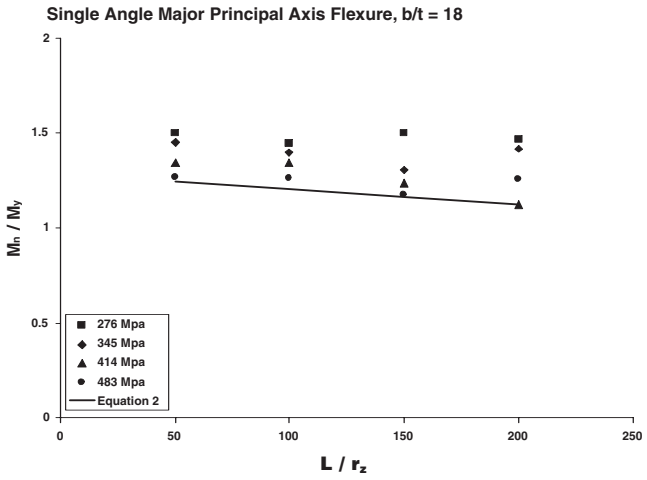

Fig. 11. Finite element results plotted with proposed predictive equation.

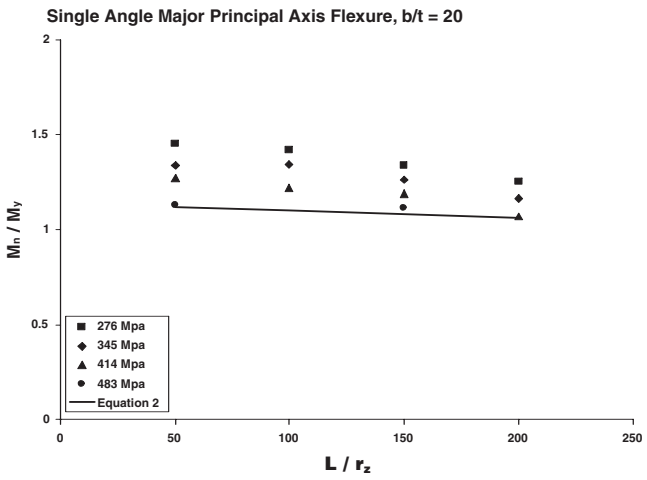

Fig. 12. Finite element results plotted with proposed predictive equation.

(indeed, inflection points oftentimes do not even exist when the buckling mode is highly localized as is frequently the case for practically useful slendernesses of single angle beams) consideration of effective length factors other than unity may not be constructive (Earls, 2002).

CONCLUSIONS

Nonlinear finite element modeling techniques have been employed herein for the study of equal-leg, hot-rolled steel single angle members bent about the major principal centroidal axis. Results from the modeling indicate that a lower bound design approach can be encapsulated in the form of two, linear, nominal moment predictive equations that depend on the angle leg slenderness (b/t) and the angle beam overall slenderness (L_b/r_z). This design approach has been shown to somewhat conservatively span the design space:

$$6 \le \frac{b}{t} \le 20, \quad 50 \le \frac{L_b}{r_z} \le 200, \quad 276\,\text{MPa} \le F_y \le 483\,\text{MPa}$$

REFERENCES

ABAQUS (1999), *ABAQUS Theory Manual*, Hibbitt, Karlsson & Sorensen, Inc., Pawtucket, Rhode Island.

AISC (2000), *Load and Resistance Factor Design Manual of Steel Construction*, Third Edition, American Institute of Steel Construction, Inc., Chicago, Illinois.

BSI (2000), *BS5950 Structural Use of Steelwork in Building. Part 1:2000, Code of Practice for Design in Simple and Continuous Construction: Hot-Rolled Sections*, British Standards Institution, London.

Earls, C.J. (1999a), "On Single Angle Major Axis Flexure," *Journal of Constructional Steel Research*, Elsevier Science Ltd., Great Britain, Vol. 51, No. 2, pp. 81-97.

Earls, C.J. (1999b), "Effects of Material Property Stratification on Single Angle Flexural Ductility," *Journal of Constructional Steel Research*, Elsevier Science Ltd., Great Britain, Vol. 51, Vol. 2, pp. 147-175.

Earls, C.J. (2001a), "Single Angle Geometric Axis Flexure, Part I: Background and Model Verification," *Journal of Constructional Steel Research*, Elsevier Science Ltd., Great Britain, Vol. 57, pp. 603-622.

Earls, C.J. (2001b), "Single Angle Geometric Axis Flexure, Part II: Design Recommendations," *Journal of Constructional Steel Research*, Elsevier Science Ltd., Great Britain, Vol. 57, pp. 623-646.

Earls, C.J. (2001c), "Single Angle Geometric Axis Flexural Compactness Criteria: Horizontal Leg Tension," *Journal of Structural Engineering*, American Society of Civil Engineers, Reston, Virginia, Vol. 127, No. 6, pp. 616-624.

Earls, C.J. (2001d), "Geometric Axis Compactness Criteria for Equal Leg Angles: Horizontal Leg Compression," *Journal of Constructional Steel Research*, Elsevier Science Ltd., Great Britain, Vol. 57, pp. 351-373.

Earls, C.J. (2002), "On the Notion of Effective Length for Single Angle Geometric Axis Flexure," *Journal of Constructional Steel Research*, Elsevier Science Ltd., Great Britain, Vol. 58, pp. 1195-1210.

Galambos, T. V. (1968), *Structural Members and Frames*, Prentice-Hall Inc., Englewood Cliffs, New Jersey, p. 108.

SA (1998), *AS 4100-1998 Steel Structures*, Standards Australia, Sydney.

Trahair, N.S. (1993), *Flexural-Torsional Buckling of Structures*, CRC Press, Boca Raton, Florida, pp. 118-157.

Trahair, N.S. (2002), "Lateral Buckling Strengths of Steel Angle Section Beams," *Research Report No. R812*, Centre for Advanced Structural Engineering, University of Sydney, Sydney, Australia.

Vlasov, V. Z. (1959), *Thin-Walled Elastic Beams*, Second Edition, Translated from Russian in 1961 by the Israel Program for Scientific Translations, Reproduced by National Technical Information Service, U.S. Department of Commerce, Springfield, Virginia.